Measurements of J/ψ decays into a vector and a pseudoscalar meson

D. Coffman, G. P. Dubois, G. Eigen, J. Hauser, D. G. Hitlin, C. G. Matthews, J. D. Richman, W. J. Wisniewski, and Y. Zhu
California Institute of Technology, Pasadena, California 91125

M. Burchell, D. E. Dorfan, J. Drinkard, C. Gatto, R. P. Hamilton,* C. A. Heusch, L. Köpke, W. S. Lockman, R. Partridge, J. Perrier, H. F. W. Sadrozinski, M. Scarlatella, T. L. Schalk, A. Seiden, A. J. Weinstein, and R. Xu
University of California at Santa Cruz, Santa Cruz, California 95064

J. J. Becker, G. T. Blaylock, B. I. Eisenstein, T. Freese, G. Gladding, J. M. Izen, S. A. Plaetzer, C. Simopoulos, A. L. Spadafora, I. E. Stockdale, J. J. Thaler, and B. Tripsas
University of Illinois at Urbana-Champaign, Urbana, Illinois 61801

U. Mallik
University of Iowa, Iowa City, Iowa 52242

J. Adler, T. Bolton, J. C. Brient, K. O. Bunnell, R. E. Cassell, D. H. Coward, K. F. Einsweiler, C. Grab, R. F. Mozley, A. Odian, D. Pitman, R. H. Schindler, W. Stockhausen, W. Toki, F. Villa, S. Wasserbaech, N. Wermes, and D. Wisinski
Stanford Linear Accelerator Center, Stanford, California 94309

J. S. Brown, T. H. Burnett, V. Cook, A. L. Duncan, A. Li, R. Mir, P. M. Mockett, B. Nemati, L. Parrish, and H. J. Willutzki
University of Washington, Seattle, Washington 98195
(Mark III Collaboration)
(Received 29 February 1988)

We present measurements of the two-body decays of the J/ψ into a vector and a pseudoscalar meson. The data, taken with the Mark III detector at the SLAC e^+e^- storage ring SPEAR, consist of 5.8×10^6 produced J/ψ's. The branching ratios for the J/ψ decays into $\rho\pi$, $\rho\eta$, $\rho\eta'$, $\omega\pi^0$, $\omega\eta$, $\omega\eta'$, $\phi\eta$, $\phi\eta'$, and K^*K are measured; an upper limit on $J/\psi\to\phi\pi^0$ is obtained. Using the measured branching ratios we obtain parameters of a phenomenological model of J/ψ decays, indicating that the η and η' are consistent with being composed only of light and strange quarks. The model is used to obtain the mixing angle in the pseudoscalar nonet. The $\omega\pi^0$ electromagnetic form factor is determined. The upper limit on $J/\psi\to\phi\pi^0$ is used to study the contributions from electromagnetic doubly-Okubo-Zweig-Iizuka-suppressed decays of the J/ψ.

I. INTRODUCTION

Decays of the J/ψ into vector-pseudoscalar (VP) meson pairs are expected to occur mainly by two mechanisms: strong decays via three-gluon annihilation [Fig. 1(a)], and electromagnetic decays through one virtual photon [Fig. 1(b)]. Electromagnetic contributions to J/ψ decays are important since the strong decays are Okubo-Zweig-Iizuka (OZI) suppressed.[1] We can, therefore, measure the isospin-violating electromagnetic decays such as $J/\psi\to\omega\pi^0$, $\rho\eta$, and $\rho\eta'$ with a sensitivity comparable to the strong decays. Diagrams with more disconnected quark lines can also contribute to the decay rates. An example is the doubly-OZI- (DOZI-) suppressed diagram [Fig. 1(c)]. Our recent analysis of $J/\psi\to\gamma\omega\phi$ decays[2] shows that DOZI-suppressed processes contribute to J/ψ decay rates. The lack of flavor correlation between the final-state mesons in the isospin-violating decay $J/\psi\to\phi\pi^0$ requires that the decay proceed via the diagram shown in Fig. 1(d). We can thus estimate the importance of this electromagnetic DOZI-suppressed diagram.

A full set of measurements of $J/\psi\to VP$ decays enables us to test the processes involved. We can study the contributions of the different amplitudes to the decay rates, the mixing angle in the pseudoscalar-meson nonet, and the quark content of its members. The pseudoscalar mixing angle and the quark content of the η and η' mesons reflect any additional contributions (e.g., gluonium or radial excitations) to the meson wave functions.[3]

Measurements of purely electromagnetic J/ψ decays can be used to calculate the electromagnetic form factors involved. These form factors are used to test QCD-inspired models of mesonic wave functions.[4] We have previously calculated electromagnetic form factors in the decays of the J/ψ to a pair of pseudoscalar mesons,[5] and

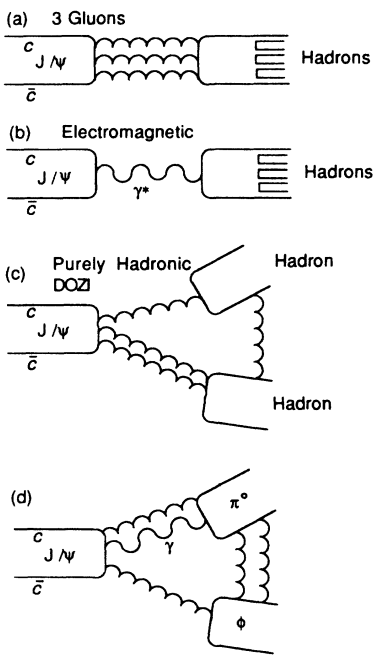

FIG. 1. Diagrams contributing to J/ψ decays: (a) three-gluon annihilation, (b) electromagnetic decay proceeding via $c\bar{c}$ annihilation into one photon, (c) a purely hadronic DOZI-suppressed decay, (d) an example of an electromagnetic DOZI-suppressed decay.

qualitative predictions have been made for their magnitude relative to the electromagnetic form factors in $J/\psi \to VP$ decays.[6] Assuming that single-photon annihilation is the dominant process in the $J/\psi \to \omega\pi^0$ decay, its electromagnetic form factor may be calculated by comparing the rate for this decay with that for the crossed-channel process $\omega \to \gamma\pi^0$.

We report herein measurements of the branching ratios for J/ψ decays to all vector (ρ, ω, ϕ, and K^*) and pseudoscalar (π, K, η, and η') meson pairs. The data set was taken with the Mark III detector at the SLAC e^+e^- storage ring SPEAR, at a center-of-mass energy equal to $m_{J/\psi}$. The data, consisting of 5.8×10^6 produced J/ψ's, were acquired in sets of 0.9×10^6, 1.8×10^6, and 3.1×10^6 J/ψ's. The number of J/ψ's in the second data set was found by studying events with 0, 1, 2, 3, and >3 charged tracks, where the trigger efficiency was determined from J/ψ decays in events of the type $\psi' \to \pi^+\pi^-\psi$ (Ref. 5). The J/ψ content of the other two data sets was found by measuring the relative rate of the $J/\psi \to \mu^+\mu^-$ decay in each period. The combined sample represents a twofold increase over the data (2.7×10^6) used in our earlier analysis of $J/\psi \to VP$ decays.[7]

In the next section we discuss the general features of event selection. The analysis features specific to each decay are presented in Sec. III. The measured branching ratios are given in Table I. In Sec. IV we investigate the physical implications of our measurements. The set of measured branching ratios is used to fit the parameters in a model of J/ψ decays which includes strong, electromagnetic, and DOZI-suppressed amplitudes. This model[8] also allows for violation of SU(3) invariance and includes a parametrization of the η and η' wave functions in terms of light and strange quarks. The mixing angle in the pseudoscalar nonet and the quark contents of the η and η' are calculated. The strength of the electromagnetic DOZI-suppressed processes is estimated. A calculation of the $\omega\pi^0$ electromagnetic form factor is performed, details of which are given in the Appendix.

II. EVENT SELECTION

The Mark III detector has been described elsewhere.[9] A brief survey follows. Photons are detected as showers in a finely segmented electromagnetic calorimeter which covers 95% of the full 4π solid angle, and is fully efficient for photon energies above 0.1 GeV. The angular resolution is 10 mrad, and the energy resolution is $\sigma_E/E = 0.17/\sqrt{E}$ (E in GeV). Charged tracks are detected in the drift chamber which covers 85% of the solid angle, and has a momentum resolution of $\sigma_p/p = 0.015\sqrt{1+p^2}$ (p in GeV/c). The time-of-flight (TOF) system covers 80% of 4π, and has a mean resolution of 200 ps, providing 3σ K/π discrimination up to 0.8 GeV/c.

The analyses of the individual channels have common features. Vector mesons are detected in the modes $\rho \to \pi^+\pi^-$, $\omega \to \pi^+\pi^-\pi^0$, $\phi \to K^+K^-$, and $K^* \to K\pi$. Pseudoscalar mesons are detected in the modes $\pi^0 \to \gamma\gamma$, $\eta \to \gamma\gamma$, $\eta \to \pi^+\pi^-\gamma$, $\eta \to \pi^+\pi^-\pi^0$, $\eta' \to \gamma\rho$, and $\eta' \to \eta\pi^+\pi^-$. Observing the η and η' decays in more than one mode allows us a cross-check of our measurements. Selection criteria on the invariant mass of a $\gamma\gamma$ pair forming a π^0 or an η differ in various decay modes. The criteria are more stringent when large backgrounds need to be suppressed. The effect on the branching ratios is included in the systematic error.

Each analysis requires events to have the correct number of charged tracks with the sum of their charges equal to zero, and at least the required number of showers. Spurious photon candidates, arising from the interactions of charged tracks in the shower counters, are minimized by rejecting showers which fall near a charged track and by imposing a minimum-energy requirement.

The selected events are kinematically fitted by imposing energy and momentum constraints. The kinematic fit adjusts the track energies and momenta within the measured errors and detector resolution, so as to satisfy the given event hypothesis. This improves the photon energy measurement and suppresses events with the wrong charged-particle assignment. When the number of showers in an event exceeds the minimum, the showers are ordered in decreasing energy, all combinations with up to three additional showers are fitted, and the combination with the minimum χ^2 is retained.

Scatter plots of the invariant mass of the vector-meson candidate versus the invariant mass of the pseudoscalar meson candidate are formed. Invariant-mass combinations which fall into the range of the V (P) meson are selected. The recoiling P (V) mass spectrum is fitted us-

ing the sum of polynomial background and a Breit-Wigner (BW) curve (width obtained from Ref. 10) convolved with a Gaussian resolution function. The number of P (V) mesons recoiling against V (P) mass sidebands is obtained by a similar fit, and is used for background subtraction.

The detection efficiency and mass resolution for each channel are found by a Monte Carlo simulation. This includes the matrix element for the $J/\psi \to VP$ decays which completely specifies the final-state angular distributions.[11] The interactions of photons in the detector are simulated using both detailed shower-simulation programs (EGS) (Ref. 12), and real photons from fully reconstructed J/ψ events.

The fractional systematic error for each branching ratio is obtained by adding contributions from the following terms in quadrature: 8.5% from the J/ψ flux, 1% from the reconstruction of each charged track, 2% from the reconstruction of each photon, 5% from the kinematic fit, 5–10 % from the selection criteria, and 5–10 % resulting from the uncertainty on the background subtraction.

III. ANALYSIS

A discussion of the analysis of each final state follows. The resulting branching ratios are given in Table I. Unless specified, the π^0 and η in the final state are identified in the $\gamma\gamma$ mode. On each result the first error is statistical and the second systematic. The average is a weighted mean of the different decay modes. The upper limit is given at the 90% confidence level.

A. $J/\psi \to \rho\pi$

The decay $J/\psi \to \rho\pi$ is observed in the $\pi^+\pi^-\gamma\gamma$ final state. The $\gamma\gamma$ invariant mass is required to be consistent with a π^0 (0.07–0.20 GeV/c^2). This removes virtually all QED backgrounds, as well as $\pi^+\pi^-\gamma$ events with an additional spurious shower. A Dalitz plot of one-third of the selected events is shown in Fig. 2. The $\rho\pi$ bands are

TABLE I. $J/\psi \to VP$ branching ratios.

Channel	Final state	Branching ratio (10^{-3})
$\rho\pi$	$\pi^+\pi^-\pi^0$	14.2±0.1±1.9
$\rho\eta$	$\pi^+\pi^-\eta$	0.191±0.013±0.034
	$\pi^+\pi^-\pi^+\pi^-\pi^0$	0.196±0.029±0.040
	Average	0.193±0.013±0.029
$\rho\eta'$	$\pi^+\pi^-\gamma\rho^0$	0.133±0.018±0.024
	$\pi^+\pi^-\eta\pi^+\pi^-$	0.097±0.022±0.017
	Average	0.114±0.014±0.016
$\omega\pi^0$	$\pi^+\pi^-\pi^0\pi^0$	0.482±0.019±0.064
$\omega\eta$	$\pi^+\pi^-\pi^0\eta$	1.86±0.06±0.25
	$\pi^+\pi^-\pi^0\gamma\pi^+\pi^-$	1.49±0.17±0.22
	Average	1.71±0.08±0.20
$\omega\eta'$	$\pi^+\pi^-\pi^0\eta\pi^+\pi^-$	0.169±0.027±0.025
	$\pi^+\pi^-\pi^0\pi^+\pi^-\pi^+\pi^-\pi^0$	0.154±0.051±0.026
	$\pi^+\pi^-\pi^0\gamma\rho^0$	0.167±0.025±0.024
	Average	0.166±0.017±0.019
$\phi\pi^0$	$K^+K^-\pi^0$	<0.0068
$\phi\eta$	$K^+K^-\eta$	0.651±0.049±0.092
	$K^+K^-\pi^+\pi^-\pi^0$	0.677±0.088±0.096
	Average	0.661±0.045±0.078
$\phi\eta'$	$K^+K^-\eta\pi^+\pi^-$	0.290±0.050±0.039
	$K^+K^-\gamma\rho^0$	0.327±0.046±0.049
	Average	0.308±0.034±0.036
$K^{*+}K^- + \text{c.c.}$	$K^\pm\pi^\mp K_S^0$	5.16±0.16±0.54
	$K^+K^-\pi^0$	5.66±0.12±0.83
	Average	5.26±0.13±0.53
$K^{*0}\bar{K}^0 + \text{c.c.}$	$K^\pm\pi^\mp K_S^0$	4.33±0.12±0.45

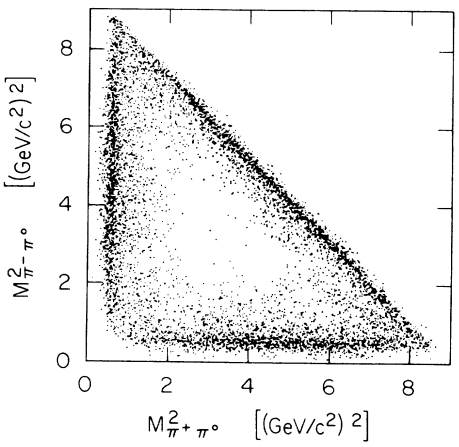

FIG. 2. The Dalitz plot for $J/\psi\to\pi^+\pi^-\pi^0$. (To emphasize the structure only one-third of the data is displayed.)

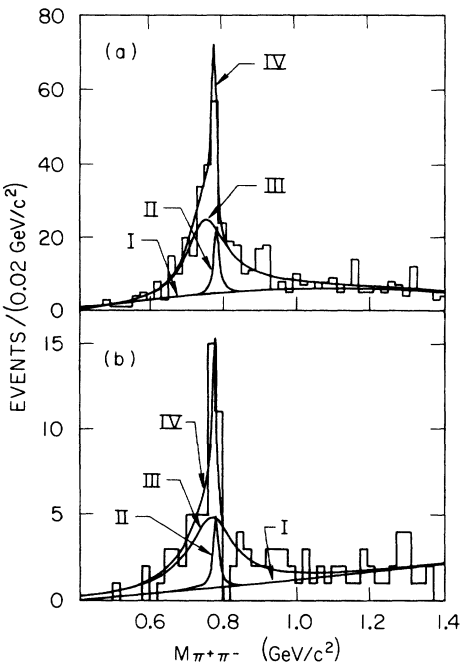

FIG. 3. The $\pi^+\pi^-$ invariant mass for events of the type $J/\psi\to\pi^+\pi^-\eta$ in the modes (a) $\eta\to\gamma\gamma$, (b) $\eta\to\pi^+\pi^-\pi^0$. The curves show the fit results for the background (I), background + ω (II), background + ρ (III), and background + ω + ρ + interference term (IV). The background is quadratic for (a), linear for (b).

dominant.[13] A study of the population in the Dalitz plot away from the $\rho\pi$ bands shows no evidence for a population uniform in phase space, or for contributions from other resonances. Possible background from another source (i.e., $J/\psi\to K^*K\to K^+K^-\pi^0$, with the kaons misidentified as pions) has been estimated by Monte Carlo simulation, and its expected contribution of (3.2±0.4)% has been subtracted from the data. We find the ratio $\rho^0\pi^0/\rho\pi$ to be 0.328±0.005±0.027, in agreement with the value of one-third expected from isospin symmetry (see Sec. IV A).

B. $J/\psi\to\rho\eta$

The decay $J/\psi\to\rho\eta$ is observed in two decay modes of the η. For the $\eta\to\gamma\gamma$ mode, events in the final state $\pi^+\pi^-\gamma\gamma$ are kinematically fitted to the hypothesis $J/\psi\to\eta\pi^+\pi^-$, where the requirement of the η mass adds an additional constraint to the fit. The $\pi^+\pi^-$ mass distribution recoiling against the η is shown in Fig. 3(a).

For the $\eta\to\pi^+\pi^-\pi^0$ mode, the final state $\pi^+\pi^-\pi^+\pi^-\gamma\gamma$ is selected. The $\gamma\gamma$ invariant mass is required to be consistent with a π^0 (0.11–0.16 GeV/c^2). All $\pi^+\pi^-\pi^0$ mass combinations consistent with an η (0.53–0.57 GeV/c^2) are considered. Only one combination per event is found in the η mass region. The $\pi^+\pi^-$ mass distribution recoiling against the η is shown in Fig. 3(b).

To obtain the number of $J/\psi\to\rho\eta$ events, the interference from the decay $J/\psi\to\omega\eta$, $\omega\to\pi^+\pi^-$ is taken into account. Although the ω decays to $\pi^+\pi^-$ with a branching ratio of only 1.7% (Ref. 10), the branching ratio for $J/\psi\to\omega\eta$ is one order of magnitude larger than that for $J/\psi\to\rho\eta$ (Table I). Interference effects are, therefore, expected to be significant. The data in Figs. 3(a) and 3(b) are fitted with the function

$$N(M_{\pi^+\pi^-})=L(M_{\pi^+\pi^-}) + |A_\rho(M_{\pi^+\pi^-})+A_\omega(M_{\pi^+\pi^-})e^{i\phi}|^2,$$

where L is a polynomial background term and A_ρ is the contribution of the $\rho\eta$ channel to the data. The amplitude $A_\rho=(N_\rho)^{1/2}F_\rho^{\rm BW}(M_{\pi^+\pi^-})$, where $F_\rho^{\rm BW}$ is the appropriate Breit-Wigner term.[13] The amplitude A_ω is similarly defined. In the fitting procedure, N_ρ, N_ω, and ϕ (the relative phase) are all left free. For the $\eta\to\gamma\gamma$ mode we find $\phi=(46\pm15)°$, the branching ratio for $J/\psi\to\rho\eta$ given in Table I, and a branching ratio for $J/\psi\to\omega\eta$ of $(1.35\pm0.14\pm0.34)\times10^{-3}$, in reasonable agreement with that measured in the $\omega\to\pi^+\pi^-\pi^0$ mode (Table I). The fit results for the $\eta\to\pi^+\pi^-\pi^0$ mode agree within errors.

C. $J/\psi\to\rho\eta'$

The decay $J/\psi\to\rho\eta'$ is observed in two decay modes of the η'. For the $\eta'\to\gamma\rho$ mode, the final state $\pi^+\pi^-\pi^+\pi^-\gamma$ is selected. Background coming from $J/\psi\to\pi^+\pi^-\pi^+\pi^-\pi^0$ is suppressed by rejecting events consistent with the five-pion hypothesis, as determined using a five-constraint (5C) fit. Figure 4(a) shows the invariant mass of the $\gamma\rho$ ($0.50<M_{\pi^+\pi^-}<0.85$ GeV/c^2) (Ref. 14) recoiling against the other ρ ($0.60<M_{\pi^+\pi^-}<0.90$ GeV/c^2) in the event. All possible $\pi^+\pi^-$ combinations consistent with two ρ's are considered. Up to four entries per event are allowed. A clear η' signal is apparent over a large background. The background comes from wrong $\pi^+\pi^-$ combinations, from the radiative decay $J/\psi\to\gamma\rho\rho$ (Ref. 15), and from residual $J/\psi\to\pi^+\pi^-\pi^+\pi^-\pi^0$ events. The $\gamma\rho$ events recoiling against ρ mass sidebands ($0.2<M_{\pi^+\pi^-}<0.4$ and

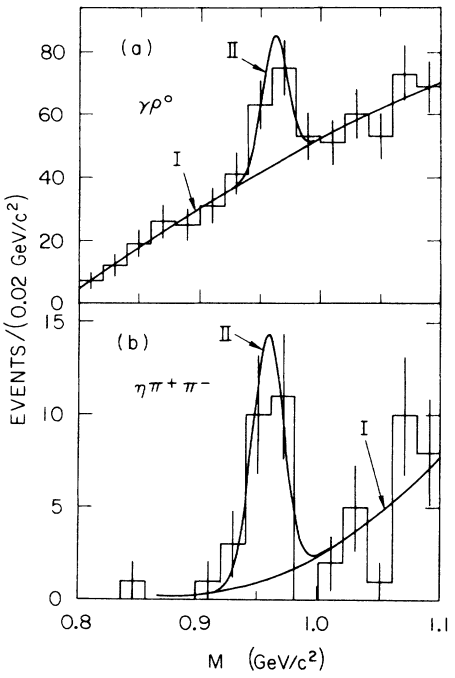

FIG. 4. (a) The $\gamma\rho$ invariant mass for events of the type $J/\psi\to\rho\rho\gamma$. (b) The $\eta\pi^+\pi^-$ invariant mass for events of the type $J/\psi\to\rho\eta\pi^+\pi^-$. The curves show the quadratic background (I) and background + η' (II).

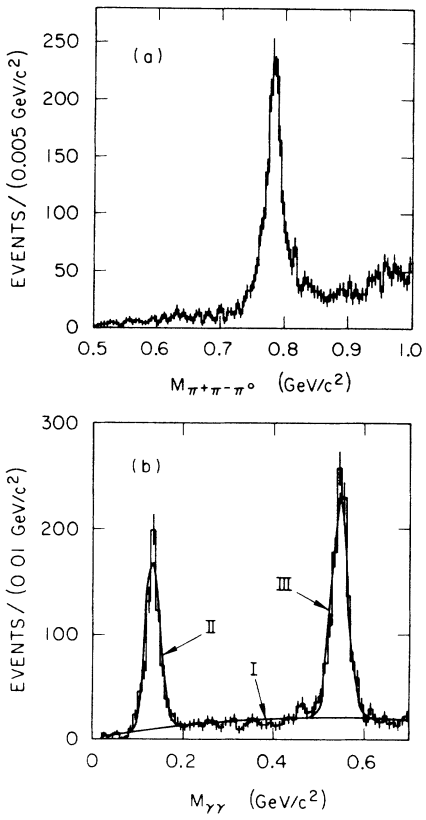

FIG. 5. (a) The $\pi^+\pi^-\pi^0$ invariant mass for events of the type $J/\psi\to\pi^+\pi^-\pi^0\gamma\gamma$. (b) The $\gamma\gamma$ invariant mass for events of the type $J/\psi\to\omega\gamma\gamma$; the curves show the quadratic background (I), background + π^0 (II), and background + η (III).

$1.2<M_{\pi^+\pi^-}<1.5$ GeV/c^2) show no significant η' signal.

For the $\eta'\to\eta\pi^+\pi^-$ mode, the final state $\pi^+\pi^-\pi^+\pi^-\gamma\gamma$ is selected. The $\gamma\gamma$ mass is required to be consistent with an η (0.53–0.57 GeV/c^2). All $\pi^+\pi^-$ mass combinations consistent with a ρ (0.60–1.00 GeV/c^2) are considered. Figure 4(b) shows the invariant mass of the $\eta\pi^+\pi^-$ events recoiling against the ρ. Only one combination per event is found in the η' mass region. A clear η' signal is apparent, well separated from the background. The ρ mass sidebands show no significant η' signal.

The possible contribution to $\rho\eta'$ from $\omega\eta'$, $\omega\to\pi^+\pi^-$ is estimated to be (5±3)% using our measured rate for $J/\psi\to\omega\eta'$ given in Table I. The data are corrected for this effect.

D. $J/\psi\to\omega\pi^0$ and $J/\psi\to\omega\eta$

The decays $J/\psi\to\omega\pi^0$ and $J/\psi\to\omega\eta$ are observed in the $\pi^+\pi^-\gamma\gamma\gamma\gamma$ final state. If at least one π^0 is found from any $\gamma\gamma$ pair ($0.10<M_{\gamma\gamma}<0.17$ GeV/c^2), the $\pi^+\pi^-\pi^0$ invariant mass [Fig. 5(a)] is formed. Events with $0.73<M_{\pi^+\pi^-\pi^0}<0.83$ GeV/c^2 are selected as ω candidates. This procedure is the same in all $J/\psi\to\omega P$ channels. The $\gamma\gamma$ invariant mass recoiling against the ω is shown in Fig. 5(b). Clear π^0 and η signals are apparent. The $\gamma\gamma$ combinations recoiling against ω mass sidebands ($0.66<M_{\pi^+\pi^-\pi^0}<0.72$ and $0.85<M_{\pi^+\pi^-\pi^0}<0.90$ GeV/c^2) are used for background subtraction.

The decay $J/\psi\to\omega\eta$ is also observed in the $\pi^+\pi^-\pi^+\pi^-\gamma\gamma\gamma$ final state. The $\gamma\pi^+\pi^-$ invariant mass recoiling against the ω is shown in Fig. 6(a). A clear η signal is seen. Curve III in Fig. 6(a) shows the Monte Carlo simulation of this signal. The branching ratio is determined by taking the total number of events in the η mass region ($0.50<M_{\gamma\pi^+\pi^-}<0.60$ GeV/c^2) and subtracting both an estimate of the phase-space background, and the contribution from $\eta\to\pi^+\pi^-\pi^0$, where one of the photons from the π^0 decay is not detected. This contribution, which populates the mass region from 0.35 to 0.50 GeV/c^2, is well reproduced by a Monte Carlo simulation [curve II in Fig. 6(a)]. The $\gamma\pi^+\pi^-$ events recoiling against ω mass sidebands are used for background subtraction.

E. $J/\psi\to\omega\eta'$

The decay $J/\psi\to\omega\eta'$ is observed in two decay modes of the η'. For the $\eta'\to\gamma\rho$ mode the final state $\pi^+\pi^-\pi^+\pi^-\gamma\gamma\gamma$ is selected. The $\gamma\pi^+\pi^-$ invariant mass recoiling against the ω is shown in Fig. 6(b), where the $\pi^+\pi^-$ invariant mass is required to be consistent with a ρ ($0.50<M_{\pi^+\pi^-}<0.90$ GeV/c^2). The ω mass sidebands show no significant η' signal.

For the $\eta'\to\eta\pi^+\pi^-$ decays, two decay modes of the η are observed. In the $\eta\to\gamma\gamma$ mode the final state

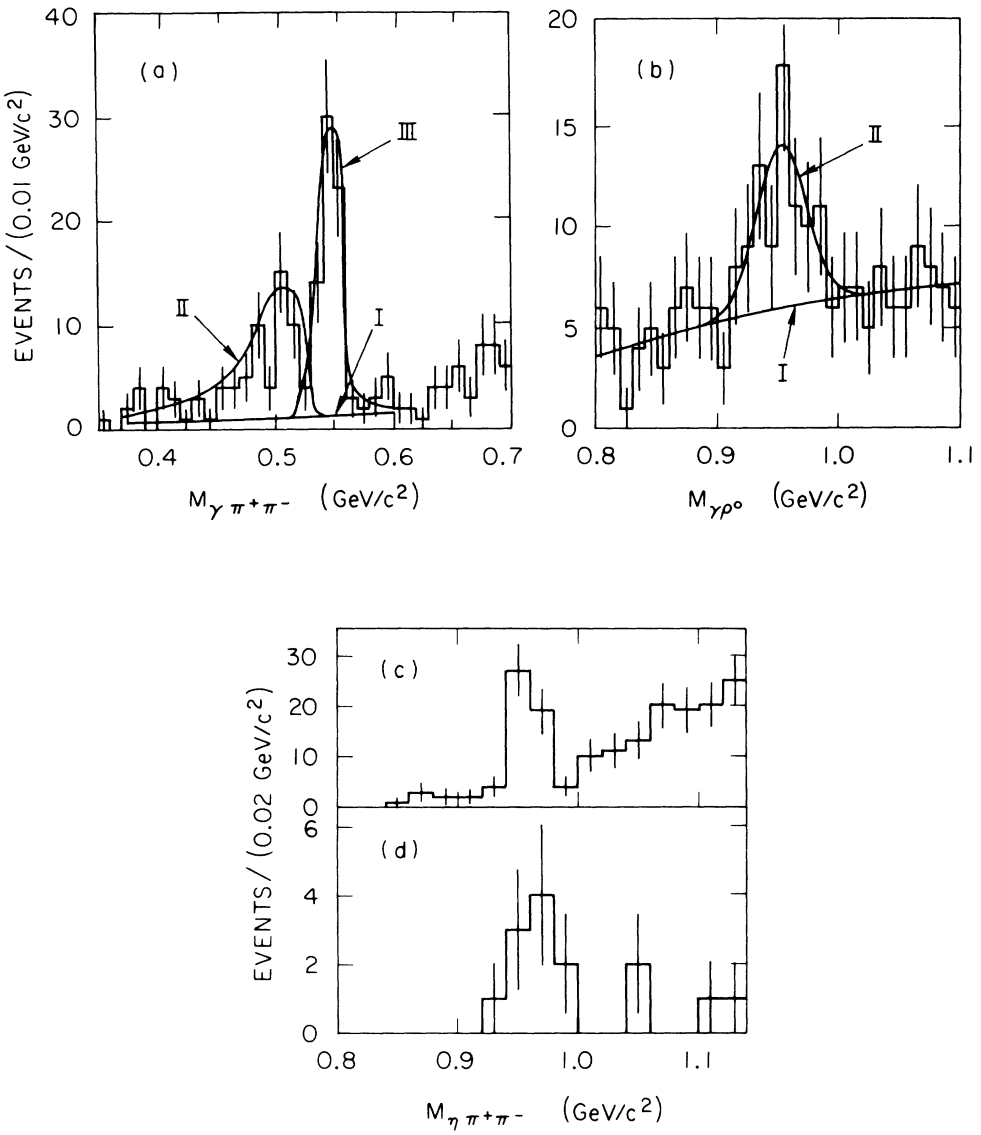

FIG. 6. (a) The $\gamma\pi^+\pi^-$ invariant mass in events of the type $J/\psi\to\omega\pi^+\pi^-\gamma$. The curves show the estimated phase-space background (I), background + Monte Carlo simulation of the decay $J/\psi\to\omega\eta$, $\eta\to\pi^+\pi^-\pi^0$ (II), and background + Monte Carlo simulation of the decay $J/\psi\to\omega\eta$, $\eta\to\pi^+\pi^-\gamma$ (III). (b) The $\gamma\rho$ invariant mass in events of the type $J/\psi\to\omega\rho\gamma$. The curves show the quadratic background (I) and the background + η' (II). (c) The $\eta\pi^+\pi^-$ invariant mass in events of the type $J/\psi\to\omega\eta\pi^+\pi^-$, $\eta\to\gamma\gamma$. (d) The $\eta\pi^+\pi^-$ invariant mass in events of the type $J/\psi\to\omega\eta\pi^+\pi^-$, $\eta\to\pi^+\pi^-\pi^0$.

$\pi^+\pi^-\pi^+\pi^-\gamma\gamma\gamma\gamma$ is selected. Following the ω selection, the other $\gamma\gamma$ invariant mass is required to be consistent with an η (0.52–0.57 GeV/c^2). The $\eta\pi^+\pi^-$ invariant mass recoiling against the ω is shown in Fig. 6(c). The ω mass sidebands are used for background subtraction. In the $\eta\to\pi^+\pi^-\pi^0$ mode the final state $\pi^+\pi^-\pi^+\pi^-\pi^+\pi^-\gamma\gamma\gamma\gamma$ is selected. Following the ω selection, the other $\gamma\gamma$ invariant mass is required to be consistent with a π^0 (0.08–0.20 GeV/c^2), and the $\pi^+\pi^-\pi^0$ invariant mass is required to be consistent with an η (0.53–0.57 GeV/c^2). The $\eta\pi^+\pi^-$ invariant mass recoiling against the ω is shown in Fig. 6(d). The number of $\omega\eta'$ events is obtained by subtracting an estimated phase-space background. The ω mass sidebands are used for background subtraction.

F. $J/\psi\to\phi\pi^0$ and $J/\psi\to\phi\eta$

The decays $J/\psi\to\phi\pi^0$ and $J/\psi\to\phi\eta$ are searched for in the $K^+K^-\gamma\gamma$ final state. The kaons have relatively low momentum and are easily separated from pions by the time-of-flight (TOF) system. The invariant mass of the two kaons recoiling against the η is shown in Fig. 7(a). Events with $1.005<M_{K^+K^-}<1.035$ GeV/c^2 are selected to be ϕ candidates. This procedure is used in all $J/\psi\to\phi P$ channels. The $\gamma\gamma$ invariant mass recoiling against the ϕ is shown in Fig. 7(b). A clear η signal is seen. The $\gamma\gamma$ events recoiling against ϕ mass sidebands ($0.98<M_{K^+K^-}<1.00$ and $1.05<M_{K^+K^-}<1.09$ GeV/c^2) are used for background subtraction.

No π^0 is visible. An analysis of the population distri-

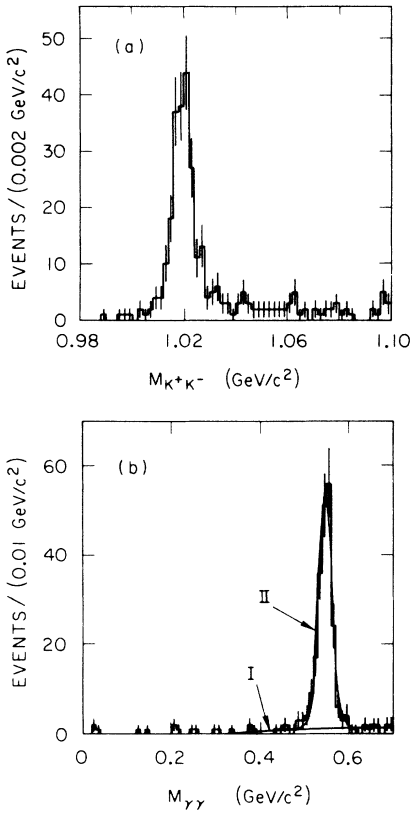

FIG. 7. (a) The K^+K^- invariant mass in events of the type $J/\psi\to K^+K^-\eta$. (b) The $\gamma\gamma$ invariant mass in events of the type $J/\psi\to\phi\gamma\gamma$; the curves show the quadratic background (I) and the background + η (II).

bution in a scatter plot of $M_{K^+K^-}$ vs $M_{\gamma\gamma}$ predicts 3.5 ± 0.5 background events in the region of the π^0 mass. Two events are observed in this region. A 90% confidence-level upper limit on the $B(J/\psi\to\phi\pi^0)$ is given in Table I (Ref. 16).

The decay $J/\psi\to\phi\eta$ is also seen in the $K^+K^-\pi^+\pi^-\gamma\gamma$ final state. Following the ϕ and π^0 ($0.08<M_{\gamma\gamma}<0.20$ GeV/c^2) selection, the $\pi^+\pi^-\pi^0$ invariant mass is shown in Fig. 8(a). The ϕ mass sidebands are used for background subtraction.

G. $J/\psi\to\phi\eta'$

The decay $J/\psi\to\phi\eta'$ is observed in two decay modes of the η'. For the $\eta'\to\gamma\rho$ mode the final state $K^+K^-\pi^+\pi^-\gamma$ is selected. Following the ϕ and ρ ($0.50<M_{\pi^+\pi^-}<0.90$ GeV/c^2) selection, the $\gamma\rho$ invariant mass recoiling against the ϕ is shown in Fig. 8(b). The ϕ mass sidebands show no η' signal.

For the $\eta'\to\eta\pi^+\pi^-$ mode the final state $K^+K^-\pi^+\pi^-\gamma\gamma$ is selected. Following the ϕ and η selection ($0.50<M_{\gamma\gamma}<0.60$ GeV/c^2), the $\eta\pi^+\pi^-$ invariant mass recoiling against the ϕ is shown in Fig. 8(c). The number of η' events is taken as the number of entries in Fig. 8(c), there being no background below 1.1 GeV/c^2. The ϕ mass sidebands are used for background subtraction.

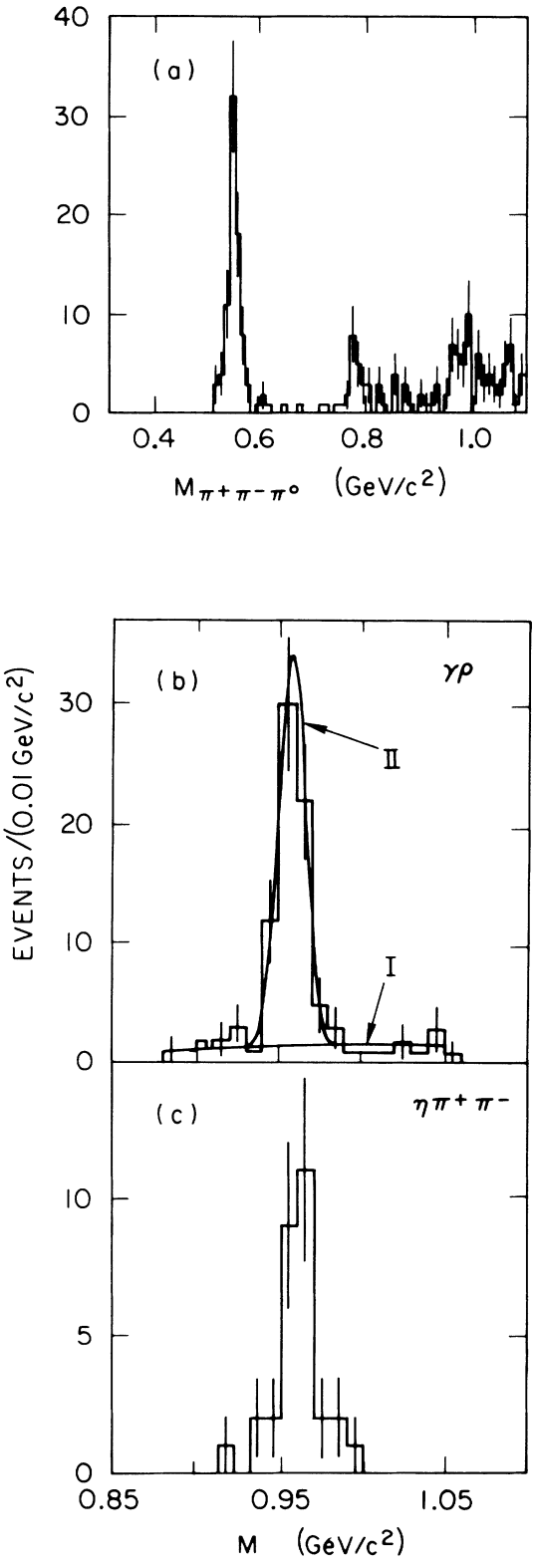

FIG. 8. (a) The $\pi^+\pi^-\pi^0$ invariant mass in events of the type $J/\psi\to\phi\pi^+\pi^-\pi^0$. (b) The $\gamma\rho$ invariant mass in events of the type $J/\psi\to\phi\rho\gamma$. The curves show the quadratic background (I) and the background + η' (II). (c) The $\eta\pi^+\pi^-$ invariant mass in events of the type $J/\psi\to\phi\eta\pi^+\pi^-$, $\eta\to\gamma\gamma$.

H. $J/\psi \to K^* K$

The decay $J/\psi \to K^* K$ is observed in the channels $K^{*\pm} K^{\mp}$ ($K^{*\pm} \to K^{\pm}\pi^0$, $K^{*\pm} \to K^0_S \pi^{\pm}$) and $K^{*0}\bar{K}^0_S$ ($K^{*0} \to K^{\pm}\pi^{\mp}$). The K^0_S is seen in the $\pi^+\pi^-$ decay mode. Events are required to have at least one kaon identified by the TOF system. In the $K^+K^-\pi^0$ mode events are rejected if they have a charged track unambiguously identified as a pion, or if the K^+K^- invariant mass is consistent with a ϕ. The latter criteria rejects only events with $M_{K^{\pm}\pi^0} > 1.4$ GeV/c^2, leaving the K^*K signal unaffected. All the final states are shown in the Dalitz plots of Fig. 9. To obtain the number of K^*K events, projections onto the mass axes are taken, and a BW curve with a quadratic background is fitted to the data.

Even though the 4C kinematic fit to $J/\psi \to \gamma\gamma K^+K^-$ rejects $J/\psi \to \gamma\gamma\pi^+\pi^-$ events, a sizable contamination from $J/\psi \to \rho\pi$ remains in the data. Such events are indistinguishable from $J/\psi \to K^*K \to K^+K^-\pi^0$, and are, therefore, simulated by Monte Carlo programs. The predicted contribution which amounts to (28±4)% of the events in the signal region is subtracted. The resulting branching ratio for $J/\psi \to K^{*\pm}K^{\mp}$ in the $K^+K^-\pi^0$ final state, given in Table I, is in good agreement with that measured in the $K^{\pm}K^0_S\pi^{\mp}$ final state. As a further check on the accuracy of the $\rho\pi$ subtraction the analysis of the $K^+K^-\pi^0$ final state is repeated with more stringent TOF selection criteria. These criteria require both charged tracks in an event to be identified as kaons, with the momentum of the kaon originating from the K^* decay to be <0.8 GeV/c. These criteria reduce the detection efficiency from 20 to 4.8%. The resulting branching ratio for $J/\psi \to K^{*\pm}K^{\mp}$ is $(5.57\pm0.25\pm0.78)\times10^{-3}$. This is in good agreement with the result in Table I, albeit with a larger statistical error.

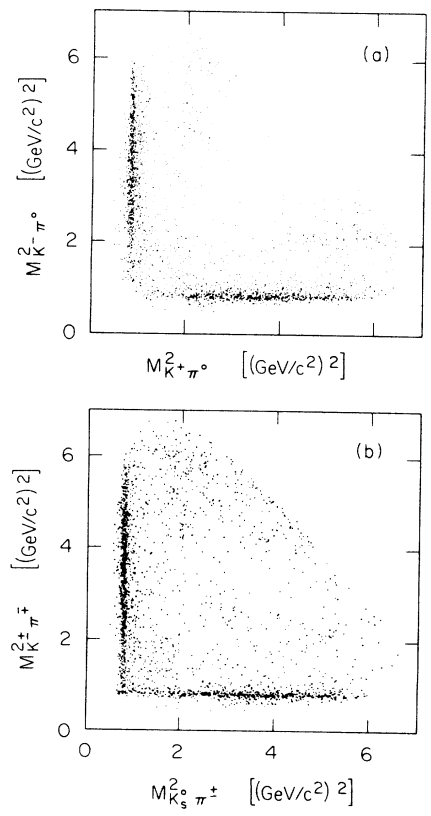

FIG. 9. (a) The Dalitz plot for $J/\psi \to K^{\pm}K^{\mp}\pi^0$. (b) The Dalitz plot for $J/\psi \to K^{\pm}\pi^+\pi^-\pi^{\mp}$ events.

IV. DISCUSSION OF RESULTS

The branching ratios $J/\psi \to VP$ are given in Table I. The results show a greater statistical accuracy than the previous Mark III measurements,[7] reflecting the increase in the number of J/ψ decays studied. The previous limit on $J/\psi \to \rho\eta'$, $\eta' \to \eta\pi^+\pi^-$ is superseded by a measurement using two decay modes of the η'. Because of the limited statisitics upon which the previous result was based (three events in the η' mass region) the background estimation was difficult. The current luminosity and improvements in the analysis method (raising the detection efficiency from 9% to 21%) provide us with a clear signal over a well-estimated background. The rate for $J/\psi \to \omega\eta'$, previously measured in two modes (one with only four events) is now measured in three modes which yield consistent branching ratios, although the value for the $\eta' \to \gamma\rho$ mode is smaller than the previous measurement by 3.7 times the previous systematic error. The branching ratio for $J/\psi \to \omega\pi^0$ measured here is lower than the old result by 1.7 times the previous systematic error, due to a better estimate of the background obtained by fitting the recoiling mass distribution rather than the recoiling momentum spectrum.

Except for the above-mentioned changes, the set of new branching ratios given in Table I agrees with the previous measurements within 1σ of the previous statistical error.

The decays of the J/ψ (being a $c\bar{c}$ quark state with well-defined initial quantum numbers) are an excellent laboratory for the study of hadron dynamics. The electromagnetic decays play an important role here because of the OZI suppression of hadronic decays via three gluons. This allows us to study $J/\psi \to VP$ decay rates in terms of the diagrams shown in Figs. 1(a) and 1(b). The influence of diagrams with more disconnected quark lines, such as the DOZI processes shown in Figs. 1(c) and 1(d), is also investigated. Further, given that the vector-meson quark assignments are well established, our measurements are used to study the quark content of the η and η' pseudoscalar mesons.

A. The mixing angle of the η and η' mesons

The widths of J/ψ into VP meson pairs can be written as

$$\Gamma(J/\psi \to VP)_i = |A_i|^2 p^3_{V_i} ,$$

where p_{V_i} is the momentum of the vector meson in the rest frame of the J/ψ.

We analyze our data using a recent phenomenological model,[8] which differs from that used to analyze our earlier measurements by including a term representing

DOZI-suppressed processes and by not requiring a gluonium contribution. Within this model the amplitudes A_i are coupled with strength g for the strong decays, rg for DOZI-suppressed processes, sg for possible SU(3) violations, and e for electromagnetic processes. These constants are relatively real, and the phase of e relative to g is defined to be θ_e.

Within the pseudoscalar nonet the η and η' mesons can be parametrized by their normalized wave functions in terms of only light and strange quarks:[3]

$$|\eta\rangle = X_\eta \frac{1}{\sqrt{2}} |u\bar{u}+d\bar{d}\rangle + Y_\eta |s\bar{s}\rangle ,$$

$$|\eta'\rangle = X_{\eta'} \frac{1}{\sqrt{2}} |u\bar{u}+d\bar{d}\rangle + Y_{\eta'} |s\bar{s}\rangle .$$

The pseudoscalar mixing angle θ_P can be written in terms of the quark content of the η and η' mesons:[17]

$$\tan\theta_P = -\frac{\sqrt{2}X_\eta + Y_\eta}{X_\eta - \sqrt{2}Y_\eta} = \frac{X_{\eta'} - \sqrt{2}Y_{\eta'}}{\sqrt{2}X_{\eta'} + Y_{\eta'}} .$$

The expected contributions of the various processes to the $J/\psi \to VP$ amplitudes in the model are given in Table II. The measured reduced branching ratios $\tilde{B} \equiv B/p_V^3$ are also given in Table II, where common systematic errors due to the normalization have been removed, and the statistical and systematic errors are added in quadrature. The predicted decay amplitudes for J/ψ decays to the variously charged $\rho\pi$ states are equal, reflecting the similar $u\bar{u}$,$d\bar{d}$ quark nature of these states. Our results (Sec. III A) are in good agreement with this prediction. By contrast, the amplitudes for J/ψ decays to neutral and charged K^*K's differ due to the different quark content of the neutral ($d\bar{s}$) and charged ($u\bar{s}$) states. This leads to differing electromagnetic contributions to the amplitudes. The necessity for such an isospin-violating effect has been noted by several authors.[18] Our model predicts that the ratio of neutral over charged K^*K's from $J/\psi \to K^*K$ should be less than 1. From our results in Table I we find this ratio to be $0.82\pm0.05\pm0.09$, in qualitative agreement with the prediction.

We fit the phenomenological model to the ten reduced branching ratios with the constraints $X_i^2 + Y_i^2 = 1$ and $X_{\eta'} = -Y_\eta$. The fit yields (with a χ^2 of 10.1 for 4 degrees of freedom)

$$X_\eta = 0.814\pm0.014, \quad g = 1.10\pm0.04 ,$$

$$s = 0.12\pm0.03, \quad \theta_e = (72\pm7)^\circ ,$$

$$e = 0.12\pm0.01, \quad r = -0.15\pm0.01 .$$

This gives $Y_\eta = -0.581$ and $\theta_P = (-19.2\pm1.4)^\circ$. The result for θ_P is in good agreement with recent two-photon results.[19]

A fit to the data, without the above constraints on X_i and Y_i yields (with a χ^2 of 0.02 for 1 degree of freedom)

$$X_\eta^2 + Y_\eta^2 = 1.00\pm0.16 \text{ and } X_{\eta'}^2 + Y_{\eta'}^2 = 1.44\pm0.26 .$$

The values of all the components describing the amplitudes are within the errors of the previous fit results. Varying the magnitudes of the reduced branching ratios to account for possible correlated systematic effects in photon reconstruction efficiencies changes the results for $X_i^2 + Y_i^2$ within the above errors.

The results of the unconstrained fit indicate that the model where the η and η' consist of only u, d, and s quarks, with no contribution from gluonium, is consistent with the data. Furthermore, the results of the constrained fit are consistent with mixing between the ground-state octet and singlet states only.

The constrained fit yields a DOZI-suppressed contribution of 15% of the OZI-violating amplitude. Using the same model with no DOZI-suppressed contribution ($r = 0$), an unconstrainted fit to the data gives a χ^2 of 25.1 for 2 degrees of freedom. A constrained fit to the data gives a χ^2 of 221.0 for 5 degrees of freedom. Setting $r = 0$ one expects $\tilde{B}(J/\psi \to \omega\eta)/\tilde{B}(J/\psi \to \omega\eta')$ to be equal to $\tilde{B}(J/\psi \to \rho\eta)/\tilde{B}(J/\psi - \rho\eta')$. The values for these ratios from Table II are 8.0 and 1.3, respectively. This illustrates the need for a DOZI-suppressed contribution in this model.

B. Contributions from electromagnetic DOZI-suppressed processes

In the model used in the previous section the nature of the DOZI-suppressed processes was assumed to be hadronic, and any electromagnetic DOZI-suppressed processes were assumed to be suppressed by at least α (the fine-structure constant). This hypothesis can be tested by considering the decay $J/\psi \to \phi\pi^0$. Unlike the other

TABLE II. Amplitudes and reduced branching ratios for $J/\psi \to VP$.

Process $J/\psi \to$	Amplitude	$\tilde{B}(10^{-3})$
$\rho^+\pi^-,\rho^0\pi^0,\rho^-\pi^+$	$g+e$	1.556±0.161
$K^{*+}K^-,K^{*-}K^+$	$g(1-s)+e$	1.017±0.061
$K^{*0}\bar{K}^0,\bar{K}^{*0}K^0$	$g(1-s)-2e$	0.836±0.055
$\omega\eta$	$(g+e)X_\eta + \sqrt{2}rg(\sqrt{2}X_\eta + Y_\eta)$	0.632±0.058
$\omega\eta'$	$(g+e)X_{\eta'} + \sqrt{2}rg(\sqrt{2}X_{\eta'} + Y_{\eta'})$	0.079±0.010
$\phi\eta$	$[g(1-2s)-2e]Y_\eta + rg(\sqrt{2}X_\eta + Y_\eta)$	0.287±0.031
$\phi\eta'$	$[g(1-2s)-2e]Y_{\eta'} + rg(\sqrt{2}X_{\eta'} + Y_{\eta'})$	0.182±0.025
$\rho^0\eta$	$3eX_\eta$	0.071±0.010
$\rho^0\eta'$	$3eX_{\eta'}$	0.054±0.009
$\omega\pi^0$	$3e$	0.159±0.017
$\phi\pi^0$	0	<0.0026

$J/\psi \to VP$ decays, it cannot proceed via any of the processes, shown in Fig. 1. It could proceed via an electromagnetic DOZI-suppressed decay, the lowest-order diagram being shown in Fig. 1(d). The upper limit on $\bar{B}(J/\psi \to \phi\pi^0)$ (Table II) is 1–2 orders of magnitude smaller than the reduced branching ratios for all other $J/\psi \to VP$ decays. This indicates that the electromagnetic DOZI-suppressed process shown in Fig. 1(d) plays a negligible role in $J/\psi \to VP$ decays.

C. The $\omega\pi^0$ electromagnetic form factor

The electromagnetic form factors for the decay of the J/ψ to two pseudoscalar mesons (such as $\pi\pi$ or KK) have been measured previously.[5] For $J/\psi \to VP$, the electromagnetic form factor $f(q^2)$ of the $\omega\pi^0$ channel is calculated here. This decay is chosen because, unlike the $\rho\eta$ and $\rho\eta'$ decays, the amplitude depends only on e, and a good measurement of the crossed-channel amplitude $\omega \to \gamma\pi^0$ exists. The ratio of electromagnetic form factors at $q^2 = m^2_{J/\psi}$ and at $q^2 = 0$ is given by (see the Appendix)

$$\frac{|f(m^2_{J/\psi})|^2}{|f(0)|^2} = \frac{\alpha}{3}\left[\frac{p_\gamma}{p_\omega}\right]^3 \frac{m_{J/\psi}\Gamma(J/\psi \to \omega\pi^0)}{\Gamma(\omega \to \gamma\pi^0)\Gamma(J/\psi \to \mu^+\mu^-)} .$$

Using the branching ratio for $J/\psi \to \omega\pi^0$ (Table I) and taking all other quantities from Ref. 10, we have

$$\frac{|f(m^2_{J/\psi})|}{|f(0)|} = 0.0335 \pm 0.0059 ,$$

in agreement with our previous determination.[7] This value is three times smaller than that for the $\pi\pi$ electromagnetic-form-factor ratio in J/ψ decay.[5] This suppression is in quantitative agreement with that predicted by hadronic helicity conservation in QCD (Ref. 20).

V. SUMMARY

New measurements for two-body decays of the J/ψ into $\rho\pi$, $\rho\eta$, $\rho\eta'$, $\omega\pi^0$, $\omega\eta$, $\omega\eta'$, $\phi\eta$, $\phi\eta'$, and K^*K, as well as a new upper limit on $\phi\pi^0$ are presented. A fit to the data using a phenomenological model requires a hadronic DOZI-suppressed contribution. The magnitude of the DOZI-suppressed contribution is (15±1)% of the OZI-violating amplitude. In this model the η and η' are found to be composed of only light and strange quarks. This rules out any gluonium contribution to the η' wave function. Using the results of the model the pseudoscalar mixing angle is found to be $\theta_P = (-19.2 \pm 1.4)°$. The decay $J/\psi \to \phi\pi^0$ is suppressed relative to the other decays, suggesting the absence of electromagnetic DOZI-suppressed contributions. The $\omega\pi^0$ electromagnetic-form-factor ratio is calculated to be $|f(m^2_{J/\psi})|/|f(0)| = 0.0335 \pm 0.0059$.

ACKNOWLEDGMENTS

We gratefully acknowledge the dedicated effort of SPEAR and the Linear Accelerator operating staff. This work was supported in part by the U.S. National Science Foundation and the U.S. Department of Energy under Contract Nos. DE-AC03-76SF00515, DE-AC02-76ER01195, DE-AC03-81ER40050, and DE-AM03-76SF00034.

APPENDIX

The matrix element for the decay $J/\psi \to \omega\pi^0$ is written as the product of two factors $\langle \omega\pi^0 | J_\mu | 0 \rangle$ and $\langle 0 | J_\mu | J/\psi \rangle$. We calculate

$$\langle \omega\pi^0 | J_\mu | 0 \rangle = f(q^2)\epsilon_{\mu\nu\sigma\rho} e^\nu_\omega p^\sigma_\omega p^\rho_\pi$$

and

$$\langle 0 | J_\mu | J/\psi \rangle = \sqrt{\alpha} g e^\mu_{J/\psi} ,$$

where $q^2 = m^2_{J/\psi}$, α is the fine-structure constant, g is the coupling constant of the J/ψ to the virtual photon, $e_i(p_i)$ is the polarization (momentum) four-vector of particle i, and $f(q^2)$ is the electromagnetic form factor. In terms of the matrix element and two-body phase space, the decay width for $J/\psi \to \omega\pi^0$ is

$$\Gamma(J/\psi \to \omega\pi^0) = \tfrac{4}{3}\pi\alpha^2 g^2 p^3_\omega |f(m^2_{J/\psi})|^2 ,$$

where p_ω is the momentum of the ω in the rest frame of the J/ψ.

The decay $J/\psi \to \mu^+\mu^-$ is used to obtain g. In the approximation $m^2_\mu \ll m^2_{J/\psi}$, we have[21]

$$\Gamma(J/\psi \to \mu^+\mu^-) = \tfrac{4}{3}\pi\alpha^2 g^2 m_{J/\psi} .$$

To normalize the electromagnetic form factor to that of $q^2 = 0$, we use the crossed process $\omega \to \gamma\pi^0$. The matrix element for this is

$$\langle \pi^0 | J_\mu | \omega \rangle = f(0)\epsilon_{\mu\nu\sigma\rho} e^\mu_\gamma e^\nu_\omega p^\sigma_\omega p^\rho_\pi ,$$

which gives

$$\Gamma(\omega \to \gamma\pi^0) = \frac{\alpha}{3} p^3_\gamma |f(0)|^2 ,$$

where p_γ is the momentum of the γ in the rest frame of the ω. We thus obtain

$$\frac{|f(m^2_{J/\psi})|^2}{|f(0)|^2} = \frac{\alpha}{3}\left[\frac{p_\gamma}{p_\omega}\right]^3 \frac{m_{J/\psi}\Gamma(J/\psi \to \omega\pi^0)}{\Gamma(\omega \to \gamma\pi^0)\Gamma(J/\psi \to \mu^+\mu^-)} .$$

---

*Deceased.

[1] S. Okubo, Phys. Lett. **5**, 165 (1963); G. Zweig, CERN Reports Nos. TH 401 and 412, 1964 (unpublished); J. Iizuka, Prog. Theor. Phys. Suppl. **37-38**, 21 (1966).

[2] G. Eigen, in *Proceedings of the 17th Symposium on Multiparticle Dynamics*, Seewinkel, Austria, 1986, edited by M. Markytan, W. Majerooto, and J. MacNaughton (World Scientific, Singapore, 1987).

[3] See, for example, H. J. Lipkin, Phys. Lett. **67B**, 65 (1977); J. L. Rosner, Phys. Rev. D **27**, 1101 (1983), and Refs. 4–15 therein.

[4]G. B. Lepage *et al.*, in *Particles and Fields—2,* proceedings of the Banff Summer Institute, Banff, Canada, 1981, edited by A. Z. Capri and A. N. Kamal (Plenum, New York, 1983), p. 83, and references therein; S. J. Brodsky *et al.*, *ibid.*, p. 143, and references therein.

[5]R. M. Baltrusaitis *et al.*, Phys. Rev. D **32**, 566 (1985).

[6]S. J. Brodsky and G. P. Lepage, Phys. Rev. D **24**, 2848 (1981).

[7]R. M. Baltrusaitis *et al.*, Phys. Rev. D **32**, 2883 (1985).

[8]A. Seiden, H. Sadrozinski, and H. Haber, in *Proceedings of the European Physical Society High Energy Physics Conference [International Europhysics Conference on High Energy Physics],* Uppsala, Sweden, 1987, edited by O. Botner (European Physical Society, Geneva, Switzerland, 1987); Phys. Rev. D **38**, 824 (1988).

[9]D. Bernstein *et al.*, Nucl. Instrum. Methods **226**, 301 (1984).

[10]Particle Data Group, M. Aguilar-Benitez *et al.*, Phys. Lett. **170B**, 1 (1986).

[11]The angular distribution $J/\psi \rightarrow VP$ is given by

$$\frac{d^3\sigma}{d\cos\theta_V d\cos\theta_1 d\phi_1} \propto \sin^2\theta_1[1+\cos^2\theta_V+\sin^2\theta_V\cos(2\phi_1)] ,$$

where θ_V is the angle between the vector meson and the positron direction, and θ_1 and ϕ_1 describe the decay products of the vector meson in its helicity frame. For example, in the three-body decays of the ω, θ_1 and ϕ_1 are the angles between the normal to the decay plane and the helicity direction. To fully describe an event, an isotropic distribution from the decay of the pseudoscalar meson is assumed.

[12]R. L. Ford and W. R. Nelson, SLAC Report No. 210, 1978 (unpublished).

[13]The shape of the ρ is described by a relativistic Breit-Wigner curve, cut off above 1.4 GeV/c^2, with a width

$$\Gamma=\Gamma_0\frac{m_0}{m}\frac{1+r^2p_0^2}{1+r^2p^2}\left[\frac{p}{p_0}\right]^3 ,$$

where m and p are the mass and momentum of the $\pi^+\pi^-$ system. Γ_0, m_0, and p_0 are taken from Ref. 10. A value of $r=3$ $(\mathrm{GeV}/c)^{-1}$ best describes the data.

[14]The mass of the ρ coming from the η' decay is shifted downward, as expected for a magnetic dipole transition.

[15]R. M. Baltrusaitis *et al.*, Phys. Rev. D **33**, 1222 (1986).

[16]The probability of obtaining the experimental result N, if the signal is between n and $n+dn$ and the expected mean background is b, is $L(n)=Ne^{-(b+n)}(b+n)^N/N!$ The upper limit at a given confidence level is obtained as described by L. Lyons, *Probability and Statistics for Nuclear and Particle Physicists* (Cambridge University Press, Cambridge, England, 1986), pp. 78–80.

[17]R. Kauffman and F. J. Gilman, Phys. Rev. D **36**, 2761 (1987).

[18]S. Rudaz, Phys. Rev. D **14**, 298 (1976); H. Kowalski and T. F. Walsh, *ibid.* **14**, 852 (1976).

[19]J. Olsson, in *Lepton and Photon Interactions,* proceedings of the International Symposium on Lepton and Photon Interactions at High Energies, Hamburg, West Germany, 1987, edited by R. Rueckl and W. Bartel [Nucl. Phys. B, Proc. Suppl. **3** (1987)]; A. Seiden, in *Photon-Photon Collisions,* proceedings of the Seventh International Workshop, Paris, France, 1986, edited by A. Courau and P. Kessler (World Scientific, Singapore, 1986); H. Aihara *et al.*, Phys. Rev. Lett. **57**, 2500 (1986).

[20]The coupling of the π^0 and ω via a single form factor gives the ω helicity to be $\lambda_\omega=\pm1$. However, momentum conservation and the QCD prediction of hadronic helicity conservation predicts $\lambda_{\pi^0}=\lambda_\omega=0$ in e^+e^- collisions. See Ref. 6.

[21]H. Pilkuhn, *Relativistic Particle Physics* (Springer, New York, 1979), pp. 169–176.